

1 **Improved one-phase model of uniform corrosion for**
2 **predicting volume of rust**

3

4 **Yanlong Zhang, PhD student**

5 Department of Civil Engineering, The University of Hong Kong, Pokfulam Road, Hong Kong, PRC

6 <https://orcid.org/0000-0003-1422-2846>

7 **Ray Kai Leung Su, Associate professor**

8 Department of Civil Engineering, The University of Hong Kong, Pokfulam Road, Hong Kong, PRC

9 (corresponding author: Tel.:+852 2859 2648; email: klsu@hku.hk)

10 <https://orcid.org/0000-0003-1052-3190>

11 This date of this paper is written: 06/08/2018

12 Number of words in the main text (excluding abstract and references): **3311**

13 Number of figures: 6

14

15 **Abstract:** One-phase models of rebar corrosion have been widely used by practicing
16 engineers to predict the volume of rust and the time to cracking of the concrete cover,
17 but the models have only considered the deformation of concrete and not the
18 deformation of steel or the rust layer. However, neglect of the deformation of the rust
19 layer may result in inaccurate predictions. This study therefore proposes an

20 adjustment factor to take into account the effect of the deformation of the rust layer on
21 predicting the volume of rust with a conventional one-phase model of uniform
22 corrosion. Furthermore, the effects of the material properties of the rust layer and
23 corrosion-induced expansive pressure on the adjustment factor are investigated. To
24 avoid inaccurate predictions of the volume of rust, the proposed adjustment factor
25 should be applied in the conventional one-phase model of corrosion when the Young's
26 modulus of rust is less than 460 MPa.

27

28 **Notation**

29 E_{rust} is the Young's modulus of rust

30 K_{rust} is the bulk modulus of rust

31 d_f is the free-expansion deformation of the steel-rust composite

32 d_c is the expansion deformation of the steel-rust under restraining pressure

33 d_s is the sum of the deformation of the steel and rust layer caused by the
34 restraining pressure

35 d_{s1} is the deformations of the rebar

36 d_{s2} is the deformations of the rust

37 P_{rust} is the corrosion-induced expansive pressure on the surrounding concrete

38 D is the initial diameter of the rebar,

- 39 d_r is the thickness of the corroded steel bar that takes into consideration the
- 40 deformation of the rust layer
- 41 E_{steel} is the Young's modulus of the steel
- 42 ν_{steel} is the Poisson's ratio of the steel
- 43 P_{rust1} is the restraining pressure of the inside of rust layer
- 44 P_{rust2} is the restraining pressure of the outside of rust layer
- 45 ν_{rust} is the Poisson's ratio of rust
- 46 V_{deform} is the volume of rust associated with the deformation of the rust layer
- 47 β is the ratio of the volume of rust to consumed steel
- 48 d_0 is the thickness of the porous zone.
- 49 V_{rust} is the total volume of rust
- 50 $V_{rust,1}$ is the volume of rust obtained from a conventional one-phase model of
- 51 uniform corrosion
- 52 $V_{deform1}$ is the deformation volume of rust associated with the conventional one-phase
- 53 model
- 54 η is the adjustment factor
- 55 $P_{rust,c}$ is the critical expansive pressure
- 56
- 57

58 **Keywords:** Corrosion/ Cracks & cracking/ Modelling/ Cement/cementitious
59 materials/ Durability-related properties

60

61 **1. Introduction**

62 The corrosion of steel bars in reinforced concrete (RC) members has been
63 identified as one of the most predominant structural deterioration problems worldwide
64 (Hu et al., 2018, Zhang et al., 2018). The durability, serviceability, and strength of RC
65 structures can be severely affected by corrosion-induced damage (Ye et al., 2018,
66 Aliabdo et al., 2018, Zhang et al., 2017a). When water and oxygen are available, the
67 initiation of rebar corrosion takes place once the free chloride content or the pH in the
68 pore solution of concrete at the surface of the steel rebars reaches the threshold limit
69 (Zhu et al., 2018, Liu et al., 2017, Al-Alaily and Hassan, 2018). The penetration
70 process of chloride and carbonation oxide can be affected by the components of
71 concrete (Elgalhud et al., 2018, Silva et al., 2017) and the crack width on the cover
72 surface (Zhang et al., 2017b, Lu et al., 2017). As the volume of rust is about two to six
73 times that of corroded steel, the expansion of rust would exert pressure onto the
74 surrounding concrete. This may eventually lead to cracking, delamination and spalling
75 of the concrete cover. The deterioration process and service life of RC structures are
76 therefore influenced by the volume of rust.

77 A number of models on rebar corrosion (El Maaddawy and Soudki, 2007, Wang
78 and Liu, 2004, Berra et al., 2003, Guzmán et al., 2011, Šavija et al., 2013, Yang et al.,
79 2018) have been developed to analyze the residual service life of RC structures. These
80 models often assume that the distribution of rust and expansive pressure are uniformly
81 distributed at the steel-concrete interface. Furthermore, only the deformation of
82 concrete was considered in those models, but not the steel bars and the rust layer
83 (Chernin and Val, 2011, Zhang et al., 2017c). These one-phase models of uniform
84 corrosion have been widely used in practice due to their simple formulation and short
85 computational time.

86 As the Young's modulus of steel rebars (~200 GPa) is much higher than that of
87 concrete (about 20 – 30 GPa), the deformation of the rebars in the one-phase models
88 can be neglected as it is found to be less than 1% for typical RC slab structures by
89 Zhang and Su (Zhang and Su, 2017). On the other hand, the influence of elastic
90 deformation of the rust layer on the prediction of the volume of rust depends on the
91 Young's modulus and Poisson's ratio of rust as well as corrosion-induced expansive
92 pressure. It is worth mentioning that there is a reciprocal relationship between elastic
93 deformation due to rust and the bulk/Young's modulus of rust. When the Young's
94 modulus of rust is low, the influence of the deformation of the rust layer on the total
95 volume of rust will be very high. Previous studies (Su and Zhang, 2015, Lu et al.,

2011, Molina et al., 1993, Balafas and Burgoyne, 2010) have shown that the influence of the deformation of the rust layer on calculating the volume of rust could be neglected if the Young's modulus of rust E_{rust} or the bulk modulus of rust K_{rust} is high, for instance, $E_{\text{rust}} \geq 500$ MPa (Su and Zhang, 2015), $E_{\text{rust}} \geq 1$ GPa (Lu et al., 2011), $K_{\text{rust}} \geq 4$ GPa (Molina et al., 1993) or $K_{\text{rust}} \geq 300$ MPa (Balafas and Burgoyne, 2010). Experimental studies on the properties of rust (Suda et al., 1993, Care, 2008, Liu and Su, 2018, Zhao et al., 2012b) have shown that E_{rust} can actually vary from 10 MPa to 300 MPa which is much less than the minimum recommended threshold limit of 500 MPa. Thus deformation of the rust layer should not be neglected in conventional one-phase models of uniform corrosion (Chen and Leung, 2018).

In this study, an adjustment factor is derived to improve the prediction of the volume of rust with a conventional one-phase model of uniform corrosion. A numerical parametric study is carried out to investigate the effects of the material properties of rust and corrosion-induced expansive pressure on the adjustment factor. Furthermore, the range of Young's modulus values of rust which is applied in the modified model is also discussed.

112

113 **2. Research significance**

114 The traditional method for calculating the rust volume with its mass and density

115 does not consider the deformation of rust caused by the confinement of surrounding
116 concrete before cover cracking. Neglecting the deformation of the rust layer would be
117 incorrect for the calculation of rust volume in corrosion models. In this paper, an
118 adjustment factor is originally derived to improve the prediction of the volume of rust
119 with considering the deformation of rust for conventional one-phase model of uniform
120 corrosion. Furthermore, a parametric study is conducted to investigate the effects of
121 the material properties of the rust and corrosion-induced expansive pressure on the
122 adjustment factor. It is found that the proposed adjustment factor should be applied
123 when the Young's modulus of rust is less than 460 MPa.

124

125 **3. Adjustment factor for volume of rust**

126 In this section, the volume of rust derived from using a three-phase model of
127 uniform corrosion is first discussed. The adjustment factor for the volume of rust
128 obtained from a conventional one-phase model of uniform corrosion will then be
129 derived.

130 As shown in Fig. 1a, the expansion of rust in a corroded rebar is confined by the
131 surrounding concrete. Owing to the confinement effect, the free-expansion
132 deformation of the steel-rust composite (d_r) is reduced to (d_c). Enforcing the
133 compatibility condition on deformation in the radial direction at the

134 steel-rust-concrete interface, the following equation can be obtained:

$$135 \quad d_f = d_s + d_c \quad (1)$$

136 where d_s is the sum of the deformation of the steel and rust layer caused by the
137 restraining pressure (P_{rust}), hence,

$$138 \quad d_s = d_{s1} + d_{s2} \quad (2)$$

139 where d_{s1} and d_{s2} are the deformations of the rebar and rust as illustrated in Figs. 1b
140 and 1c, respectively.

141 As shown in Fig. 1b, the steel rebar can be treated as a plane strain problem
142 subjected to only external pressure. The deformation of the steel bar can be expressed
143 with Eq.(3) (Ugural, 1994).

$$144 \quad d_{s1} = \frac{P_{rust}(D/2-d_r)(1-\nu_{steel})}{E_{steel}} \approx \frac{P_{rust}D(1-\nu_{steel})}{2E_{steel}} \quad (3)$$

145 where P_{rust} is the corrosion-induced expansive pressure on the surrounding concrete,
146 D is the initial diameter of the rebar, d_r is the thickness of the corroded steel bar that
147 takes into consideration the deformation of the rust layer, and E_{steel} and ν_{steel} are the
148 Young's modulus and Poisson's ratio of the steel, respectively.

149 As $d_f < D$, it is reasonable to assume that the restraining pressure of the inside
150 and outside of the rust layer (P_{rust1} and P_{rust2} as shown in Fig. 1c) are the same and
151 equals to P_{rust} . Therefore, the deformation of the rust layer in the radial direction can
152 be expressed as:

153
$$d_{s2} = \frac{P_{\text{rust}}(d_f + d_r)}{K_{\text{rust}}} \quad (4)$$

154 where K_{rust} is the bulk modulus of rust. The bulk modulus of rust can be related to the
 155 Young's modulus and Poisson's ratio of rust ν_{rust} in Eq. (5).

156
$$K_{\text{rust}} = \frac{E_{\text{rust}}}{3(1-2\nu_{\text{rust}})} \quad (5)$$

157 Rust is a granular material and its structure consists of a powder grain aggregate
 158 (Ouglova et al., 2006, Liu and Su, 2018). It has been found that the Young's modulus
 159 of rust increases with an increase of expansive pressure (Liu and Su, 2018, Ouglova et
 160 al., 2006, Xu et al., 2017) or rust thickness (Care, 2008). In this study, for
 161 simplification, rust is treated as an elastic material. This assumption has been widely
 162 adopted in many analytical models (Zhao et al., 2012a, Su and Zhang, 2015, Zhu and
 163 Zi, 2017). The deformation of the rust layer when subjected to expansive pressure is
 164 illustrated in Fig. 1c. The volume of rust associated with the deformation of the rust
 165 layer (V_{deform}) can be expressed with Eq. (6).

166
$$V_{\text{deform}} = \pi d_{s2}(D + d_f) \approx \pi d_{s2}D \quad (6)$$

167 As corrosion progresses, the total volume of rust can be derived from (Su and
 168 Zhang, 2015, Zhao et al., 2011): (1) the volume of steel consumed in the corrosion
 169 process; (2) penetration of rust into the porous zone which is caused by entrapped or
 170 entrained air at the interface between the steel and concrete (Liu and Weyers, 1998),
 171 and (3) the expansive pressure induced at the steel/concrete interface. Therefore, the

172 total thickness of the rust can be determined by using:

$$173 \quad \beta d_r = d_r + d_0 + d_f \quad (7)$$

174 where β is the ratio of the volume of rust to consumed steel and d_0 is the thickness of
175 the porous zone. It should be noted that researchers have not yet reached consensus on
176 whether rust fills corrosion-induced cracks (Wong et al., 2010, Ožbolt et al., 2012,
177 Tran et al., 2011, Chernin et al., 2012) and if so, how much; thus, the amount of rust
178 in corrosion-induced cracks is not taken into account in this study.

179 The volume of rust associated with the deformation of the rust layer (V_{deform})
180 which is called the deformation volume of rust herein can be derived from Eqs. (1) to
181 (7).

$$182 \quad V_{\text{deform}} = \frac{3\pi DP_{\text{rust}}(1-2\nu_{\text{rust}})(\beta d_r - d_0)}{E_{\text{rust}}} \quad (8)$$

183 It is worth noting that in Eq. (8), P_{rust} , E_{rust} , ν_{rust} , D , β and d_0 are independent of the
184 deformation of the rust layer except for d_r .

185 The total volume of rust (V_{rust}) obtained from the three-phase model with
186 consideration of the deformation of the rust layer can be written as:

$$187 \quad V_{\text{rust}} = V_{\text{rust},1} + V_{\text{deform}} \quad (9)$$

188 where $V_{\text{rust},1}$ is the volume of rust obtained from a conventional one-phase model of
189 uniform corrosion; see Eq.(10):

$$190 \quad V_{\text{rust},1} = \pi\beta d_{r1}(D - d_{r1}) \approx \pi\beta d_{r1}D \quad (10)$$

191 where d_{r1} is the thickness of the corroded steel obtained from the conventional
 192 one-phase model. As the thickness of the corroded steel determined from the
 193 one-phase model is different from that obtained with the three-phase model, the
 194 corresponding deformation volume of rust will also change. The deformation volume
 195 of rust associated with the conventional one-phase model (V_{deform1}) is determined with
 196 Eq. (11).

$$197 \quad V_{\text{deform1}} = \frac{3\pi DP_{\text{rust}}(1-2\nu_{\text{rust}})(\beta d_{r1}-d_0)}{E_{\text{rust}}} \quad (11)$$

198 The relationship between d_r and d_{r1} is

$$199 \quad \frac{d_{r1}}{d_r} = \frac{V_{\text{rust},1}}{V_{\text{rust}}} \quad (12)$$

200 With Eqs. (1) to (12), the total volume of rust with the effect of the deformation
 201 of the rust layer can be obtained:

$$202 \quad V_{\text{rust}} = \eta V_{\text{rust},1} \quad (13)$$

203 where η is the adjustment factor for the volume of rust obtained from the conventional
 204 one-phase model of corrosion. This factor can be analytically expressed as:

$$205 \quad \eta = \frac{\beta d_{r1}-d_0 A}{\beta d_{r1}(1-A)} \quad (14)$$

206 where

$$207 \quad A = \frac{3P_{\text{rust}}(1-2\nu_{\text{rust}})(\beta d_{r1}-d_0)}{(\beta d_{r1}-d_0)E_{\text{rust}}} \quad (15)$$

208 The deformation volume and the total volume of rust vary throughout the
 209 corrosion process. The total volume of rust leading to cover cracking is a key

210 parameter for predicting the service life of RC structures. This study focuses on
211 evaluating the deformation volume and the total volume of rust associated with the
212 critical expansive pressure, $P_{rust,c}$ at which unstable cracks propagate across the
213 thickness of the cover (Su and Zhang, 2015). It should be noted that the critical
214 expansive pressure that causes cracking of the concrete cover is influenced by the
215 material properties of concrete (i.e. Young's modulus, tensile strength and tensile
216 stress-strain relationship) and the geometrical properties of the concrete cover (i.e.
217 cover thickness and reinforcing bar diameter) (Zhang and Su, 2017) but not the
218 deformation of the rust layer and rebars. This means that $P_{rust,c}$ obtained from the
219 one-phase and three-phase models of corrosion is the same.

220 In this study, $P_{rust,c}$ is determined from a three-phase model of uniform corrosion
221 by considering the following conditions: (1) the force equilibrium in the tangential
222 direction, (2) volume expansion in the steel-rust-concrete interface, (3) deformation
223 compatibility in the steel-rust-concrete interface, (4) the force equilibrium in the radial
224 direction, and (5) bilinear relationship of the tension softening curve of concrete (Su
225 and Zhang, 2015). After considering the critical pressures associated with wide ranges
226 of tensile capacities of concrete, reinforcement diameters and cover thicknesses, $P_{rust,c}$
227 is determined by the least squares method and expressed as (Zhang and Su, 2017):

228
$$P_{rust,c} = -0.00338f_t Dc + 0.11308f_t c + 0.00118D^2c - 0.03689Dc +$$

$$\begin{aligned}
& 0.02319D^2f_t - 0.68993f_tD + 3.9058f_t - 0.10141D^2 + 0.22599c + 3.0511D - \\
& \hspace{20em} 15.418 \hspace{2em} (16)
\end{aligned}$$

where f_t is the tensile strength of concrete and c is the thickness of the concrete cover.

To obtain the adjusted total volume of rust, the adjustment factor, η , should be evaluated first from Eqs. (14) and (15) in which the expansive pressure P_{rust} , and the thickness of the corroded steel d_{r1} , can be calculated from a conventional one-phase model. Then, the total volume of rust can be obtained from Eq. (13).

4. Results and discussion

4.1. Validation

Lu et al. (Lu et al., 2011) studied the influence of the Young's modulus and Poisson's ratio of rust on the volume of corroded steel. Zhao et al. (Zhao et al., 2011) developed an analytical model to simulate corrosion-induced cover cracking. When cracking took place throughout the entire cover, the deformation of the rust layer obtained by using their analytical model and through experiments is discussed in (Zhao et al., 2012c). The input parameters of the model are listed in Table 1. The corrosion-induced expansive pressure values and the thickness of the corroded steel are taken from our previous works (Zhang and Su, 2017, Su and Zhang, 2015). Fig. 2 is a comparison of the adjustment factor determined from this study and that obtained

248 by Lu et al. (Lu et al., 2011) and Zhao et al. (Zhao et al., 2011, Zhao et al., 2012c). It
 249 can be observed that the analytical results here are in good agreement with the results
 250 in Lu et al. (Lu et al., 2011) and Zhao et al. (Zhao et al., 2011, Zhao et al., 2012c).

251 **Table 1** Input parameters of model

	f_t (MPa)	c (mm)	D (mm)	d_0 (μm)	β	ν_{rust}	E_{steel} (GPa)	ν_{steel}
Ref. (Lu et al., 2011)	3.3	35	16	16	3	0.35	200	0.3
Ref. (Zhao et al., 2011, Zhao et al., 2012c)	1.96	27	16	20	2.6	0.25	200	0.3

252

253 4.2. Parametric study

254 In this section, the effects of the Young's modulus and Poisson's ratio of rust and
 255 corrosion-induced expansive pressure on the adjustment factor, η , are examined. The
 256 input parameters are the same as those in the three-phase model (Su and Zhang, 2015,
 257 Zhang and Su, 2017).

258 4.2.1 Effect of bulk modulus of rust

259 The variations in the adjustment factor, η , from the Young's modulus of rust, E_{rust} ,
 260 are provided in Fig. 3. It can be observed that with an increase in the Young's
 261 modulus of rust, the adjustment factor first substantially decreases and then is
 262 asymptotically reduced to 1, which is in agreement with Lu et al. (Lu et al., 2011) and
 263 Su and Zhang (Su and Zhang, 2015).

264 4.2.2 Effect of Poisson's ratio of rust

265 The effect of the Poisson's ratio of rust, ν_{rust} , on the adjustment factor, η , is
266 shown in Fig. 4. It can be observed that a larger Poisson's ratio of rust results in a
267 lower adjustment factor. This finding is supported by the analytical results in Lu et al.
268 (Lu et al., 2011) and Balafas and Burgoyne (Balafas and Burgoyne, 2011). The
269 reason is that a larger Poisson's ratio of rust will result in a higher bulk modulus of
270 rust and fewer errors in the prediction of the deformation of the rust layer.

271 4.2.3 Effect of expansive pressure

272 The effect of expansive pressure, P_{rust} , on the adjustment factor, η , is shown in
273 Fig. 5. It can be seen that the adjustment factor increases with an increase in the
274 expansive pressure. This is reasonable as higher expansive pressure means greater
275 deformation of the steel bars and rust layer (Zhao et al., 2011, Balafas and Burgoyne,
276 2011). Thus, the volume of rust will be greatly underestimated in the conventional
277 one-phase model of corrosion.

278

279 **5. Condition for use of proposed adjustment factor**

280 According to the parametric study in Section 3.2, the Young's modulus of rust
281 and the critical expansive pressure both have a significant influence on the adjustment
282 factor. Unfortunately, the range of the Young's modulus of rust is still unknown and a
283 wide range of values (from 10 MPa to 200 GPa) have been reported in the literature

284 (Suda et al., 1993, Care, 2008, Liu and Su, 2018, Zhao et al., 2012b, Zhao et al.,
285 2012a, Karin, 2002, Ouglova et al., 2006, Sanz et al., 2017, Chen and Leung, 2015).

286 In this section, the range of the Young's modulus values of rust that requires the use of
287 the proposed adjustment factor for accurately calculating the volume of rust is
288 examined.

289 According to Zhang and Su (Zhang and Su, 2017), the minimum critical value of
290 the expansive pressure that could cause unstable cracking of the cover of typical RC
291 structures is 5 MPa which can develop when $f_t = 2.8$ MPa, $c = 25$ mm and $D = 20$ mm.
292 On the other hand, when $f_t = 4.3$ MPa, $c = 80$ mm and $D = 12$ mm, the maximum
293 critical value of the expansive pressure will be produced. Fig. 6 shows the effect of
294 the Young's modulus of rust on the adjustment factor under the considered minimum
295 and maximum critical values of expansive pressure. It can be seen that there are two
296 cases as follows.

297 (1) When $460 \text{ MPa} \leq E_{\text{rust}}$, the adjustment factor is less than 1.05 for a typical
298 range of critical values of expansive pressure. This means that when $460 \text{ MPa} \leq E_{\text{rust}}$,
299 the conventional one-phase model can be used to calculate the volume of rust of
300 general RC structures without introducing significant errors.

301 (2) When $E_{\text{rust}} < 460 \text{ MPa}$, the adjustment factor can be greater than 1.05 for
302 some RC structures, which means that the adjustment factor should be used when

303 calculating the volume of rust.

304 Therefore, it is recommended that the proposed adjustment factor should be used
305 when the Young's modulus of rust is less than 460 MPa for general RC structures.

306

307 **6. Conclusion**

308 In this study, an adjustment factor is proposed to improve the accuracy of the
309 prediction of the volume of rust which corresponds to cracking of the concrete cover
310 obtained from a conventional one-phase model of uniform corrosion. The effects of
311 the material properties of rust (e.g. Young's modulus and Poisson's ratio) and critical
312 value of the expansive pressure on the adjustment factor are investigated. It is found
313 that the Young's modulus of rust has a significant influence on the adjustment factor.

314 This study also finds that the conventional one-phase model of corrosion can be
315 generally used for accurately calculating the volume of rust when $E_{\text{rust}} \geq 460$ MPa for
316 typical RC structures. However, when $E_{\text{rust}} < 460$ MPa, the proposed adjustment
317 factor should be used to improve the accuracy of the prediction of the volume of rust
318 determined from the conventional one-phase model of corrosion.

319 It is worth noting that although this study focuses on the effect of the deformation
320 of the rust layer based on predictions of the volume of rust with a conventional
321 one-phase model of uniform corrosion, a similar adjustment factor for the prediction

322 of the volume of rust with one-phase models of non-uniform corrosion can also be
323 derived.

324

325 **References**

- 326 AL-ALAILY, H. S. & HASSAN, A. A. A. 2018. A study on the effect of curing temperature and
327 duration on rebar corrosion. *Magazine of Concrete Research*, 70, 260-270.
- 328 ALIABDO, A. A., ABD ELMOATY, A. E. M. & MOHAMED, M. F. 2018. Permeability indices and
329 corrosion resistance of geopolymer and Portland cement concretes. *Magazine of Concrete*
330 *Research*, 70, 595-609.
- 331 BALAFAS, I. & BURGORYNE, C. J. 2011. Modeling the structural effects of rust in concrete cover.
332 *Journal of Engineering Mechanics*, 137, 175-185.
- 333 BALAFAS, I. & BURGOYNE, C. J. 2010. Environmental effects on cover cracking due to corrosion.
334 *Cement and Concrete Research*, 40, 1429-1440.
- 335 BERRA, M., CASTELLANI, A., CORONELLI, D., ZANNI, S. & ZHANG, G. 2003. Steel-concrete
336 bond deterioration due to corrosion: finite-element analysis for different confinement levels.
337 *Magazine of Concrete Research*, 55, 237-247.
- 338 CARE, S. 2008. Mechanical properties of the rust layer induced by impressed current method in
339 reinforced mortar. *Cement and Concrete Research*, 38, 1079-1091.
- 340 CHEN, E. & LEUNG, C. K. Y. 2015. Finite element modeling of concrete cover cracking due to
341 non-uniform steel corrosion. *Engineering Fracture Mechanics*, 134, 61-78.
- 342 CHEN, E. & LEUNG, C. K. Y. 2018. Mechanical aspects of simulating crack propagation in concrete
343 under steel corrosion. *Construction and Building Materials*, 191, 165-175.
- 344 CHERNIN, L., VAL, D. & STEWART, M. 2012. Prediction of cover crack propagation in RC
345 structures caused by corrosion. *Magazine of Concrete Research*, 64, 95-111.
- 346 CHERNIN, L. & VAL, D. V. 2011. Prediction of corrosion-induced cover cracking in reinforced
347 concrete structures. *Construction and Building Materials*, 25, 1854-1869.
- 348 EL MAADDAWY, T. & SOUDKI, K. 2007. A model for prediction of time from corrosion initiation to
349 corrosion cracking. *Cement and Concrete Composites*, 29, 168-175.
- 350 ELGALHUD, A., DHIR, R. & GHATAORA, G. 2018. Chloride ingress in concrete: limestone addition
351 effects. *Magazine of Concrete Research*, 70, 292-313.
- 352 GUZMÁN, S., GÁLVEZ, J. C. & SANCHO, J. M. 2011. Cover cracking of reinforced concrete due to
353 rebar corrosion induced by chloride penetration. *Cement and Concrete Research*, 41, 893-902.
- 354 HU, Z., LI-XUAN, M., XIA, J., JIANG-BIN, L., GAO, J., YANG, J. & QING-FENG, L. 2018.
355 Five-phase modelling for effective diffusion coefficient of chlorides in recycled concrete.

356 *Magazine of Concrete Research*, 70, 583-594.

357 KARIN, L. 2002. Modelling the effect of corrosion on bond in reinforced concrete. *Magazine of*
358 *Concrete Research*, 54, 165-173.

359 LIU, Q. & SU, R. K. L. 2018. A displacement-based inverse analysis method to estimate in-situ
360 Young's modulus of steel rust in reinforced concrete. *Engineering Fracture Mechanics*, 192,
361 114-128.

362 LIU, Q. F., EASTERBROOK, D., LI, L. Y. & LI, D. 2017. Prediction of chloride diffusion coefficients
363 using multi-phase models. *Magazine of Concrete Research*, 69, 134-144.

364 LIU, Y. & WEYERS, R. 1998. Modeling the time-to-corrosion cracking in chloride contaminated
365 reinforced concrete structures. *ACI Materials Journal*, 95, 675-681.

366 LU, C., JIN, W. & LIU, R. 2011. Reinforcement corrosion-induced cover cracking and its time
367 prediction for reinforced concrete structures. *Corrosion Science*, 53, 1337-1347.

368 LU, C. H., LI, H. & LIU, R. G. 2017. Chloride transport in cracked RC beams under dry-wet cycles.
369 *Magazine of Concrete Research*, 69, 453-466.

370 MOLINA, F. J., ALONSO, C. & ANDRADE, C. 1993. Cover cracking as a function of rebar corrosion:
371 Part 2—Numerical model. *Materials and Structures*, 26, 532-548.

372 OUGLOVA, A., BERTHAUD, Y., FRANÇOIS, M. & FOCT, F. 2006. Mechanical properties of an iron
373 oxide formed by corrosion in reinforced concrete structures. *Corrosion Science*, 48,
374 3988-4000.

375 OŽBOLT, J., ORŠANIĆ, F., BALABANIĆ, G. & KUŠTER, M. 2012. Modeling damage in concrete
376 caused by corrosion of reinforcement: coupled 3D FE model. *International Journal of*
377 *Fracture*, 178, 233-244.

378 SANZ, B., PLANAS, J. & SANCHO, J. M. 2017. A method to determine the constitutive parameters of
379 oxide in accelerated corrosion tests of reinforced concrete specimens. *Cement and Concrete*
380 *Research*, 101, 68-81.

381 ŠAVIJA, B., LUKOVIĆ, M., PACHECO, J. & SCHLANGEN, E. 2013. Cracking of the concrete cover
382 due to reinforcement corrosion: A two-dimensional lattice model study. *Construction and*
383 *Building Materials*, 44, 626-638.

384 SILVA, A., NEVES, R. & DE BRITO, J. 2017. Statistical modelling of the influential factors on
385 chloride penetration in concrete. *Mag. Concr. Res.*, 69, 255-270.

386 SU, R. K. L. & ZHANG, Y. 2015. A double-cylinder model incorporating confinement effects for the
387 analysis of corrosion-caused cover cracking in reinforced concrete structures. *Corrosion*
388 *Science*, 99, 205-218.

389 SUDA, K., MISRA, S. & MOTOHASHI, K. 1993. Corrosion products of reinforcing bars embedded in
390 concrete. *Corrosion Science*, 35, 1543-1549.

391 TRAN, K. K., NAKAMURA, H., KAWAMURA, K. & KUNIEDA, M. 2011. Analysis of crack
392 propagation due to rebar corrosion using RBSM. *Cement and Concrete Composites*, 33,
393 906-917.

394 UGURAL, A. C. 1994. *Advanced strength and applied elasticity*, Englewood Cliffs, N.J., Prentice Hall.

395 WANG, X. H. & LIU, X. L. 2004. Modelling effects of corrosion on cover cracking and bond in
396 reinforced concrete. *Magazine of Concrete Research*, 56, 191-199.

397 WONG, H. S., ZHAO, Y. X., KARIMI, A. R., BUENFELD, N. R. & JIN, W. L. 2010. On the
398 penetration of corrosion products from reinforcing steel into concrete due to chloride-induced
399 corrosion. *Corrosion Science*, 52, 2469-2480.

400 XU, G., LIU, L., BAO, H., WANG, Q. & ZHAO, J. 2017. Mechanical properties of steel corrosion
401 products in reinforced concrete. *Materials and Structures*, 50, 1-10.

402 YANG, S., LI, K. & CHUN-QING, L. 2018. Analytical model for non-uniform corrosion-induced
403 concrete cracking. *Magazine of Concrete Research*, 70, 1-10.

404 YE, H., FU, C., JIN, N. & JIN, X. 2018. Performance of reinforced concrete beams corroded under
405 sustained service loads: A comparative study of two accelerated corrosion techniques.
406 *Construction and Building Materials*, 162, 286-297.

407 ZHANG, J., MA, H. & LI, Z. 2017a. Steel corrosion in magnesia-phosphate cement concrete beams.
408 *Magazine of Concrete Research*, 69, 35-45.

409 ZHANG, R., JIN, L., LIU, M., DU, X. L. & LI, Y. 2017b. Numerical investigation of chloride
410 diffusivity in cracked concrete. *Magazine of Concrete Research*, 69, 850-864.

411 ZHANG, X., LI, M., TANG, L., MEMON, S. A., MA, G., XING, F. & SUN, H. 2017c. Corrosion
412 induced stress field and cracking time of reinforced concrete with initial defects: Analytical
413 modeling and experimental investigation. *Corrosion Science*, 120, 158-170.

414 ZHANG, Y. & SU, R. K. L. 2017. Concrete cover tensile capacity of corroded reinforced concrete.
415 *Construction and Building Materials*, 136, 57-64.

416 ZHANG, Y., ZHUANG, H., SHI, J., HUANG, J. & ZHANG, J. 2018. Time-dependent characteristic
417 and similarity of chloride diffusivity in concrete. *Magazine of Concrete Research*, 70,
418 129-137.

419 ZHAO, Y., DAI, H. & JIN, W. 2012a. A study of the elastic moduli of corrosion products using
420 nano-indentation techniques. *Corrosion Science*, 65, 163-168.

421 ZHAO, Y., DAI, H., REN, H. & JIN, W. 2012b. Experimental study of the modulus of steel corrosion
422 in a concrete port. *Corrosion Science*, 56, 17-25.

423 ZHAO, Y., YU, J. & JIN, W. 2011. Damage analysis and cracking model of reinforced concrete
424 structures with rebar corrosion. *Corrosion Science*, 53, 3388-3397.

425 ZHAO, Y., YU, J., WU, Y. & JIN, W. 2012c. Critical thickness of rust layer at inner and out surface
426 cracking of concrete cover in reinforced concrete structures. *Corrosion Science*, 59, 316-323.

427 ZHU, X. & ZI, G. 2017. A 2D mechano-chemical model for the simulation of reinforcement corrosion
428 and concrete damage. *Construction and Building Materials*, 137, 330-344.

429 ZHU, X., ZI, G., SUN, L. & YOU, I. 2018. A simplified probabilistic model for the combined action of
430 carbonation and chloride ingress. *Magazine of Concrete Research*, 11, 1-14.

431

432 **A list of Figures**

433 **Fig. 1.** Deformation at steel-concrete interface in three-phase model of corrosion: (a)
434 compatibility condition on deformation in radial direction; (b) deformation of steel
435 bar; (c) deformation of rust layer.

436 **Fig. 2.** Comparison of adjustment factor for volume of rust from different methods

437 **Fig. 3.** Effect of E_{rust} on η : ($v_{\text{rust}} = 0.3$, $\beta = 3$, $f_t = 3.3$ MPa, $c = 25$ mm, $D = 16$ mm, d_0
438 $= 16$ μm , $E_{\text{steel}} = 200$ GPa, $\nu_{\text{steel}} = 0.3$)

439 **Fig. 4.** Effect of ν_{rust} on η : ($E_{\text{rust}} = 1000$ MPa, $\beta = 3$, $f_t = 3.3$ MPa, $c = 51$ mm, $D = 16$
440 mm, $d_0 = 16$ μm , $E_{\text{steel}} = 200$ GPa, $\nu_{\text{steel}} = 0.3$)

441 **Fig. 5.** Effect of P_{rust} on η : ($E_{\text{rust}} = 1000$ MPa, $\nu_{\text{rust}} = 0.3$, $\beta = 3$, $d_0 = 16$ μm , $E_{\text{steel}} = 200$
442 GPa, $\nu_{\text{steel}} = 0.3$)

443 **Fig. 6.** Effect of E_{rust} on η ($\nu_{\text{rust}} = 0.3$, $\beta = 3$, $d_0 = 16$ μm , $E_{\text{steel}} = 200$ GPa, $\nu_{\text{steel}} = 0.3$)

444

445

446 **A list of Tables**

447 **Table 1** Input parameters of model

448

449

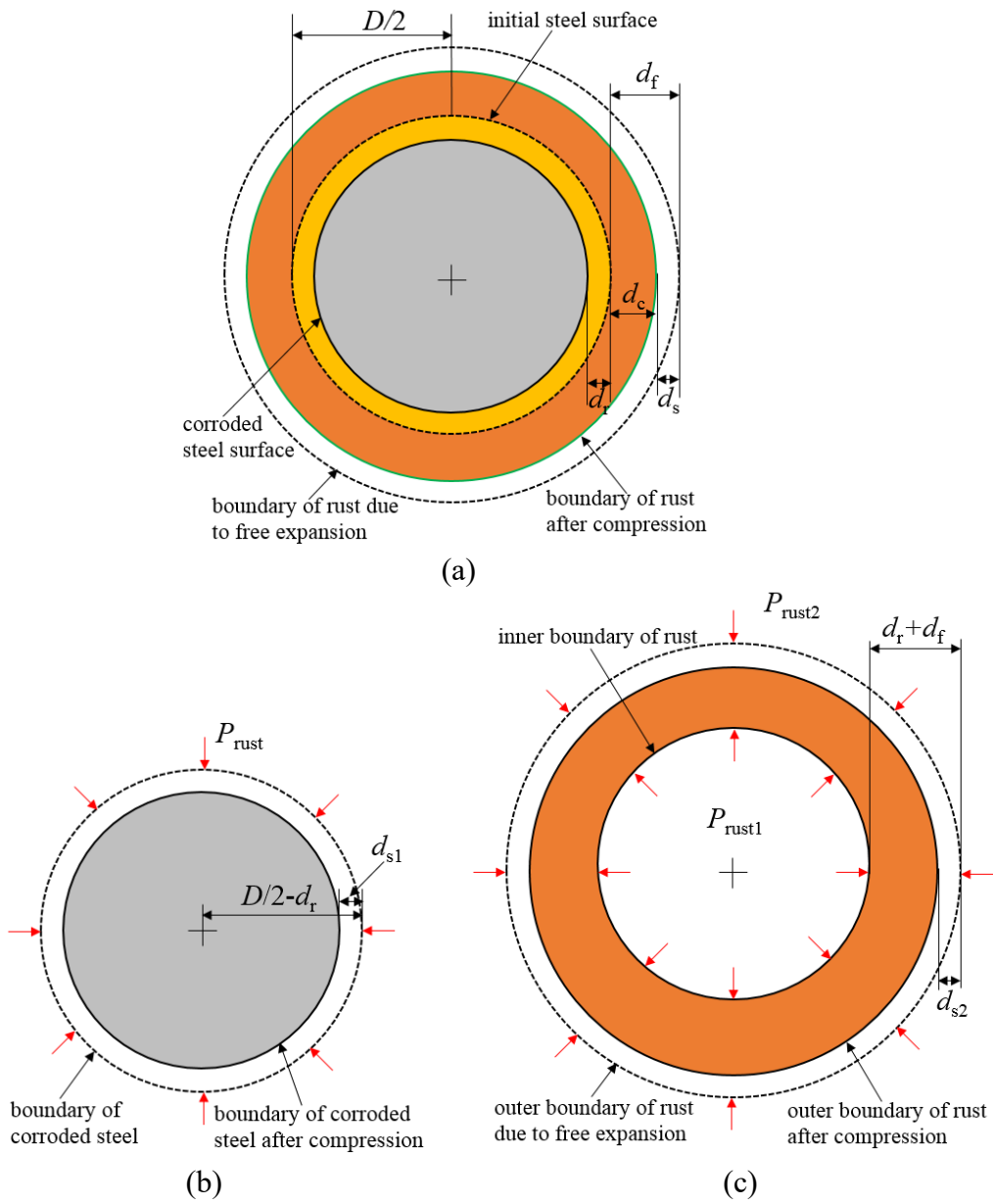
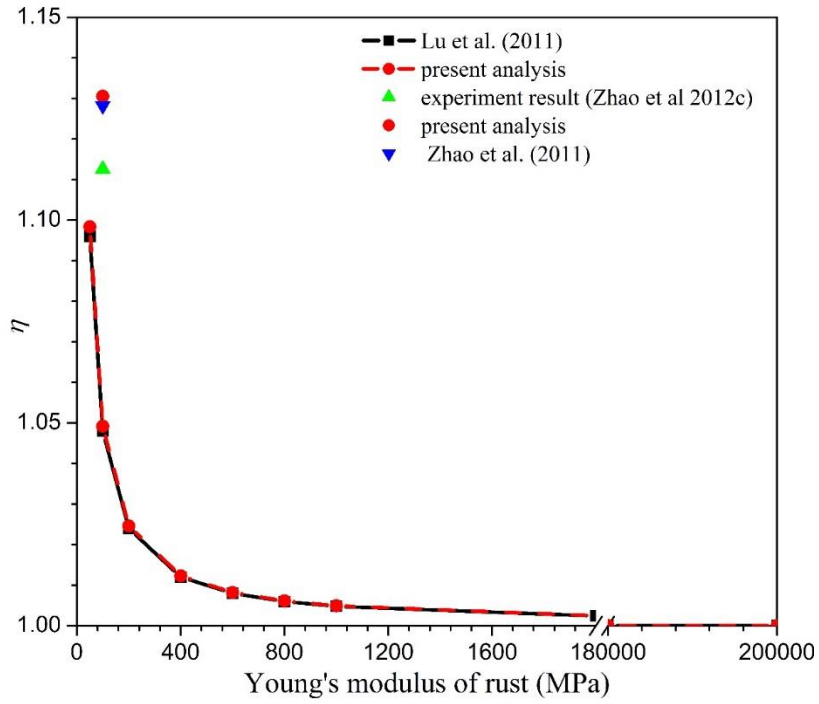
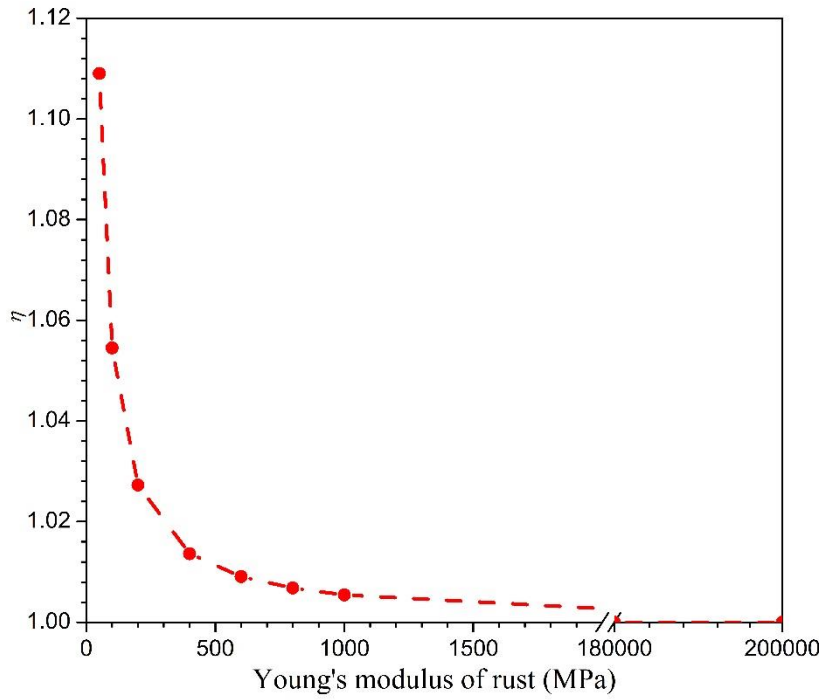


Fig 1. Deformation at steel-concrete interface in three-phase model of corrosion: (a) compatibility condition on deformation in radial direction; (b) deformation of steel bar; (c) deformation of rust layer.



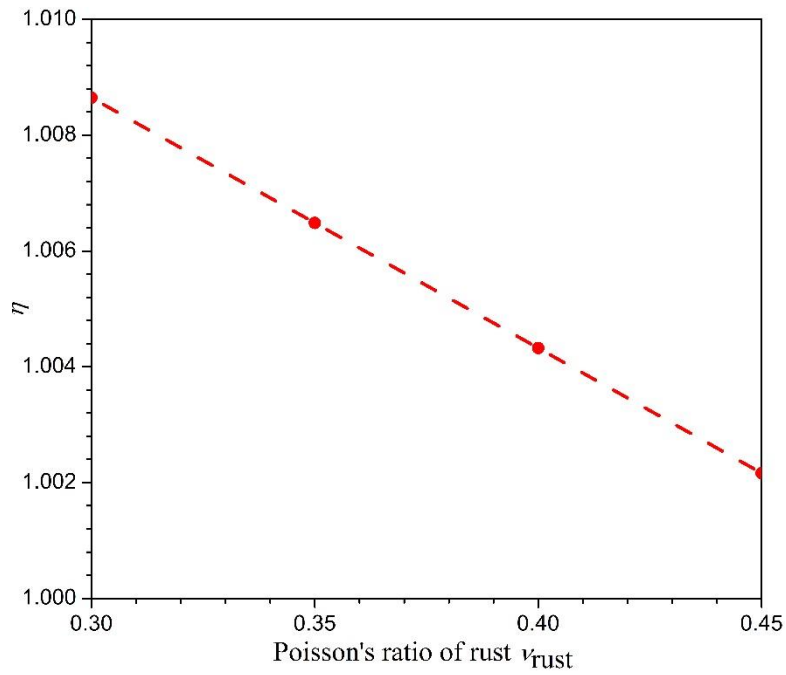
451

452 **Fig. 2.** Comparison of adjustment factor for volume of rust from different methods



453

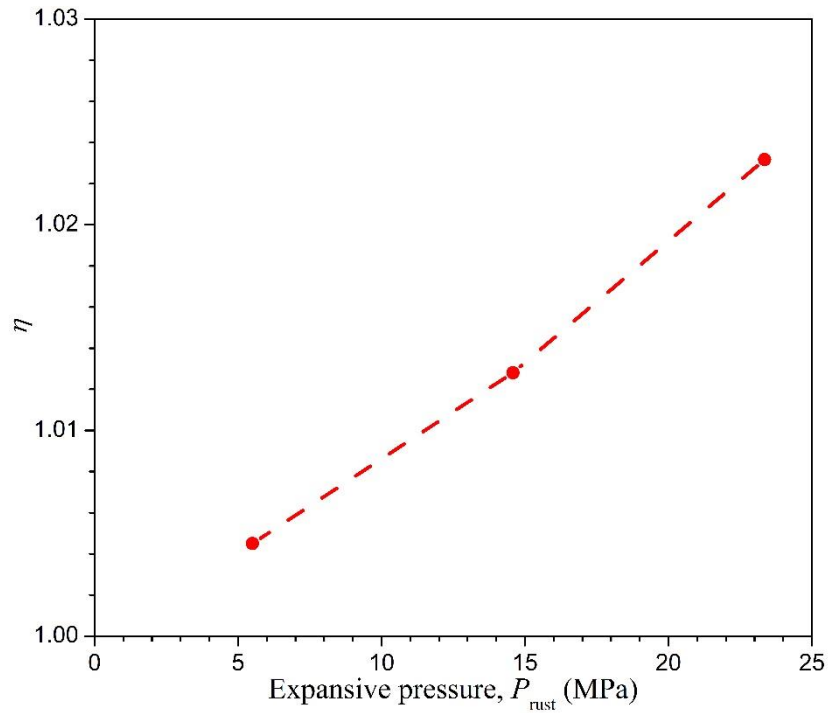
454 **Fig. 3.** Effect of E_{rust} on η : ($\nu_{rust} = 0.3$, $\beta = 3$, $f_t = 3.3$ MPa, $c = 25$ mm, $D = 16$ mm, d_0
 455 $= 16$ μ m, $E_{steel} = 200$ GPa, $\nu_{steel} = 0.3$)



456

457 **Fig. 4.** Effect of ν_{rust} on η : ($E_{rust} = 1000$ MPa, $\beta = 3$, $f_t = 3.3$ MPa, $c = 51$ mm, $D = 16$

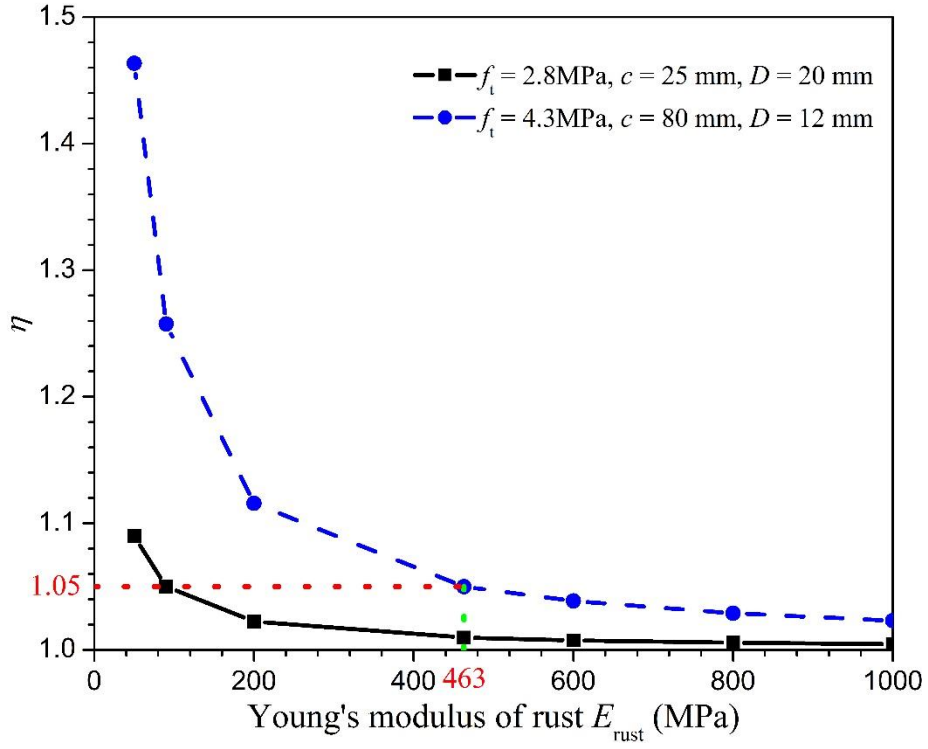
458 mm, $d_0 = 16$ μ m, $E_{steel} = 200$ GPa, $\nu_{steel} = 0.3$)



459

460 **Fig. 5.** Effect of P_{rust} on η : ($E_{rust} = 1000$ MPa, $\nu_{rust} = 0.3$, $\beta = 3$, $d_0 = 16$ μ m, $E_{steel} = 200$

461 GPa, $\nu_{steel} = 0.3$)



462

463 **Fig. 6.** Effect of E_{rust} on η ($\nu_{rust} = 0.3, \beta = 3, d_0 = 16 \mu\text{m}, E_{steel} = 200 \text{ GPa}, \nu_{steel} = 0.3$)

464